Indonesian Journal of Science & Technology

Journal homepage: http://ejournal.upi.edu/index.php/ijost/

Dye-Doped Fe_3O_4 Nanoparticles for Magnetically Controlling Random Laser Parameters at Visible Wavelengths: Literature Review and Experiment

*M. S. Al-Samak *, J. M. Jassim*

Department of Laser Physics, College of Science for Women, University of Babylon, Hillah, Iraq
* Corresponding author, email: mohammed.rahoomi@student.uobabylon.edu.iq

ABSTRACT

The development of light-controlled electronic devices requires new possibilities of optical control via tuning of laser input parameters. Here, Fe_3O_4 superparamagnetic nanoparticles (SNPs) were doped with dye, and the controllability of parameters of a random laser, including the wavelength, threshold energy, and intensity under the absence and presence of an external magnetic field was studied. The prepared dye laser (Rh-640) showed strong magnetic controllability and switch ability under different pumping energies (1–7 mJ), as well as good responsivity and durability at visible wavelengths. The applied magnetic field was utilized to modify the distribution of Fe_3O_4 SNPs with different concentrations and scattering behavior, altering the generation of coherent loops and laser action properties. Thus, it was possible to employ the magnetically controllable random laser in a variety of technological applications, including biology and optical communications.

ARTICLE INFO

Article History:
Submitted/Received 24 Jul 2022
First Revised 29 Aug 2022
Accepted 17 Oct 2022
First Available online 18 Oct 2022
Publication Date 01 Dec 2022

Keyword:
(Rh-640) dye,
Fe_3O_4 nanoparticle,
Magnetic field,
Random laser,
Tuning wavelength.

1. INTRODUCTION

Despite the conventional lasers that require a rigid optical resonator, it is possible to fabricate random lasers based on the feedback of mirror-free scattering centers (Liao *et al.,* 2017). Random lasers can be equipped with superior qualities that are difficult to be achieved using conventional lasers (Bachelard *et al.,* 2014). By representing the light amplification via stimulated emission with the feedback provided by disordered scattering, random lasers have remained an attractive topic for many researchers in the field of laser physics. These lasers have unique intrinsic properties such as simple structure and large angular emission without the need for external cavities (Ejbarah *et al.,* 2020). Therefore, great efforts have been devoted to realizing random lasers in different materials with a wide wavelength range from ultraviolet to mid-infrared and the terahertz frequency (Knitter *et al.,* 2013). Nevertheless, the mechanism of controlling the direction of the random laser emission has remained the biggest challenge for researchers in this field. While simplicity and randomness present an obstacle to the control of random lasers (Bachelard *et al.,* 2014; Kedia and Sinha 2017; Perumbilavil *et al.,* 2018), several approaches have been proposed to overcome these constraints. In this regard, three characteristics of random lasers should be taken into consideration, involving the wavelength control, laser threshold, and intensity of the emitted laser beam (Rashidi *et al.,* 2021).

The wavelength control is one of the most important advantages of a random laser. This is because of the possibility of controlling the wavelength of the random laser either through the so-called previous control, including the adjustment of the absorption state, or the appropriate selection of the size, type, and shape of the nanomaterial in addition to the shape and thickness of the cell. Alternatively, it has also been possible to control the random laser through the so-called post-control, being carried out by controlling external parameters such as the temperature, shed electric field, and optics (Ye *et al.,* 2017). As for the random laser directionality, several techniques have been utilized to control this important characteristic using optical waveguides, low-dimensional cavities, and a specific structure for the random laser (Turitsyn *et al.,* 2014; Schönhuber *et al.,* 2016; Wetter and Jimenez-Villar 2019; Kumar *et al.*, 2021).

Concerning the third characteristic, several strategies have been employed to control the laser threshold, including the use of an appropriate concentration of nanomaterial and dye mixtures, improving the size of the scattering centers and the mean free path, and tuning of the refractive index between the gain and scattering media (Meng *et al.,* 2009; Cerdán *et al.,* 2012; Lin and Hsiao 2014; Tommasi *et al.,* 2016). The fourth characteristic (the intensity of the random laser emission) has also been investigated under the influence of many factors, including the optimization of the selection of the dye and the nanomaterial, the size, and type of the nanomaterial, the concentration of both the dye and the nanomaterial, the pumping power, and the type of source (Lau *et al.,* 2005; Popov *et al.,* 2006; Wiersma 2008; Chen *et al.,* 2011; Yu 2015).

Amongst the nanomaterials, nanoparticles (NPs) with superparamagnetic behavior have become interesting because they can be easily controlled under an external magnetic field owing to their extremely low coercive field and high saturation magnetization (Chung and Fu 2011; Brojabasi *et al.,* 2015; Jing *et al.,* 2021). For example, magnetite (Fe_3O_4) superparamagnetic NPs (SNPs) have shown these features significantly (Bajpai and Gupta 2010; Koo *et al.,* 2019). In fact, at room temperature, by exceeding the Brownian rotation time over the Néel relaxation time, Fe_3O_4 SNPs lose their magnetization

DOI: https://doi.org/10.17509/ijost.v7i3.51453
p- ISSN 2528-1410 e- ISSN 2527-8045

following the removal of the magnetic field, revealing their superparamagnetic properties (Taylor *et al.*, 1986; Nguyen *et al.*, 2021). Nevertheless, these SNPs have not yet been doped with dyes to be employed in the control of random laser parameters.

In this paper, Fe_3O_4 SNPs are doped with dye (Rh-640), followed by their utilization in a random laser. Under the absence and presence of an external magnetic field, the three characteristics of the random laser (the wavelength, threshold, and intensity) are studied and discussed separately. This study gives insights into the magnetic controllability of the random laser parameters using dye-doped Fe_3O_4 SNPs.

2. LITERATURE REVIEW

Brojabasi *et al.*, (2015) studied magneto-optical transmission in ferrofluids consisting of different Fe_3O_4 NP sizes. The average diameters of Fe_3O_4 NPs were reported to be 15, 30, and 46 nm, respectively. Initially, the external field was absent, observing only a bright circular spot on the screen. The external field was then applied to the ferrofluids. By increasing the intensity of the external field, a straight-line scattering pattern with spotty parts was seen as justified by the aggregation process. This process was induced by the external field.

It was also found that the intensity of the transmitted light was enhanced in the initial state, followed by reaching a maximum value. Beyond this value, the transmitted intensity was inversely reduced as a function of field intensity, reaching a minimum value. Interestingly, decreasing the average diameters of the NPs in the ferrofluids increased both the critical field intensities to higher values. The authors attributed the observed phenomena to the formation of particle chains and column structures in the aggregation process. In other words, at a constant concentration, ferrofluids with smaller sizes of NPs required stronger field intensities to form chains of particles.

Tsai *et al.*, (2017) designed and fabricated magnetically controllable random lasers (MCRLs). Under a prescribed magnetic field (0, 1066, and 2008 Gauss), they used a random medium composed of stilbene 420 laser dye as a gain medium and a mixture of TiO_2 and Fe_3O_4 NPs as scatters. The wavelength excitation was a Q-switched Nd:YAG laser (266 nm, 3–5 ns pulse, 10 Hz). The Fe_3O_4 NPs possessed magnetic controllability due to their susceptibility with good responsivity and durability for the magnetic field.

The applied magnetic field was used to manipulate the distribution of Fe_3O_4 NPs, which in turn altered the formation of the coherent loops and the properties of laser action and provided strong optical confinement and feedback for laser action. At a zero magnetic field, the slope of spontaneous emission intensity was relatively small. With increasing the magnetic field, two thresholds were observed, reaching 12.4 and 25.4 mJ/cm^2, being above the value of the first threshold (12.1 mJ/cm^2). The results showed that the lasing threshold initially decreased to a minimum value, and was then enhanced by increasing the magnetic field. On the other hand, beyond the first threshold value, the corresponding to a Full width at half maximum (FWHM) was significantly reduced from 11.2 to 5.7 nm, representing the occurrence of amplified spontaneous emission. By further increasing the magnetic field to the second threshold (25.4 mJ/cm^2), the FWHM decreased to 0.3 nm, implying the appearance of laser action under the magnetic field effect. Thus, the lasing emission of the MCRLs can be switched on/off with great responsivity and durability by installing/removing the magnet.

Some researchers fabricated a magnetically tunable random laser (Dai *et al.*, 2019). In this case, polymer-dispersed liquid crystal (PDLC) in the capillary was achieved by employing doping magnetic NPs at varied pump energies. They used 532 nm laser pulses (10 ns &10 Hz) focused on the samples

DOI: https://doi.org/10.17509/ijost.v7i3.51453
p- ISSN 2528-1410 e- ISSN 2527-8045

with a cylindrical lens (f=20 cm). The external magnetic field was applied by a cylindrical magnet. The intensity of the magnetic field was tuned by varying the distance between the magnet and the capillary. Experimental results showed the lasing threshold was enhanced with increasing doping concentration (0, 0.01, 0.02, and 0.03 wt%) of the NPs. The respective thresholds were 9.5, 11.5, 12.3, and 18.5 μJ. As well, this effect was due to the larger absorption of NPs with a higher concentration. By increasing the applied external magnetic field, the blue shift of emission spectra was observed following an increase in the NP concentration. Furthermore, the blue shift was induced by the shorted resonator cavity, followed by a decrease in the mean free path (MFP) with an increasing concentration of NPs. Meanwhile, the dye molecules drifted away from the gain volume, resulting in a reduction in the dye concentration. Consequently, the gain length of the sample was enhanced. In addition, the decrease in the dye concentration was able to reduce self-absorption, thereby leading to the blue shift of the envelope center of the laser spectrum. Some researchers used the Fe_3O_4@SiO_2 core-shell NPs as scatters in Rhodamine B solutions (Ye *et al.,* 2015). The average diameter of the NPs was 200 nm, whereas the thickness of the SiO_2 shell was 50 nm. The pump source employed was the second harmonic of an Nd:YAG laser (532nm, 10 ns, 10 Hz). The first threshold was found to be at 100 μJ/pulse in the absence of a magnetic field. Additionally, well-separated sharp spikes with linewidth smaller than 0.2 nm appeared around 590 nm, indicating the occurrence of coherent random lasing. Nevertheless, threshold energy was reported to be 120 μJ/pulse in the presence of a magnetic field. It was because most of the NPs in the solution was effectively separated from the pump region under the application of the magnetic field. It was revealed that the Fe_3O_4@SiO_2 doped dye solution possessed a magnetically controllable feature. Also, the sharp spikes disappeared when the diameter of Fe_3O_4 NPs was relatively large (about 100 nm), whereas the laser peaks existed when the diameter of Fe_3O_4 was relatively small (about 12 nm). Accordingly, this kind of random laser had potential applications in the fabrication of magnetic sensors and integrated optical devices.

3. METHOD

3.1. Sample Preparation

The dye samples of the random laser were prepared as follows: The dye used in this experiment (Rh-640, a dark green crystal powder in appearance with a concentration of 5×10^{-4} M, purchased from Sigma Aldrich) was dissolved in methanol to obtain the laser gain medium. Afterward, Fe_3O_4 SNPs (1.3×10^{17} cm^{-3} in density, purchased from VCN materials, Iran) were mixed with the dye solution. Two samples of the random medium were then prepared by doping 70% of Rh-640 dye with 30% of Fe_3O_4 SNPs (sample-1), and 50% of Rh-640 dye with 50% of Fe_3O_4 SNPs (sample-2). These samples consisting of the dye and SNPs were ultrasonically dispersed in methanol for 30 min before each experiment.

3.2. Experimental Setup and Characterization

The experimental setup used for magnetically controlling the random laser is schematically depicted in **Figure 1**. The random suspension media were placed in a quartz cuvette with a thickness of about 10 mm at the magnetic system center and kept inside a solenoid. The magnetic field was fixed at 125 G. A Q-switched frequency-doubled Nd:YAG laser (532 nm, 5 ns pulse width, 10 Hz pulse repetition rate) was oriented at 90° concerning the normal to the cuvette face. The dye laser emission from the front face of the cuvette was collected using a lens (f = 5 cm) oriented at 30° concerning the normal to a fiber-coupled spectrometer (Ocean Optics USB2000+UV-VS-ES with a spectral resolution of ~ 0.3 nm). The direction of the magnetic field was parallel to the light propagation.

DOI: https://doi.org/10.17509/ijost.v7i3.51453
p- ISSN 2528-1410 e- ISSN 2527-8045

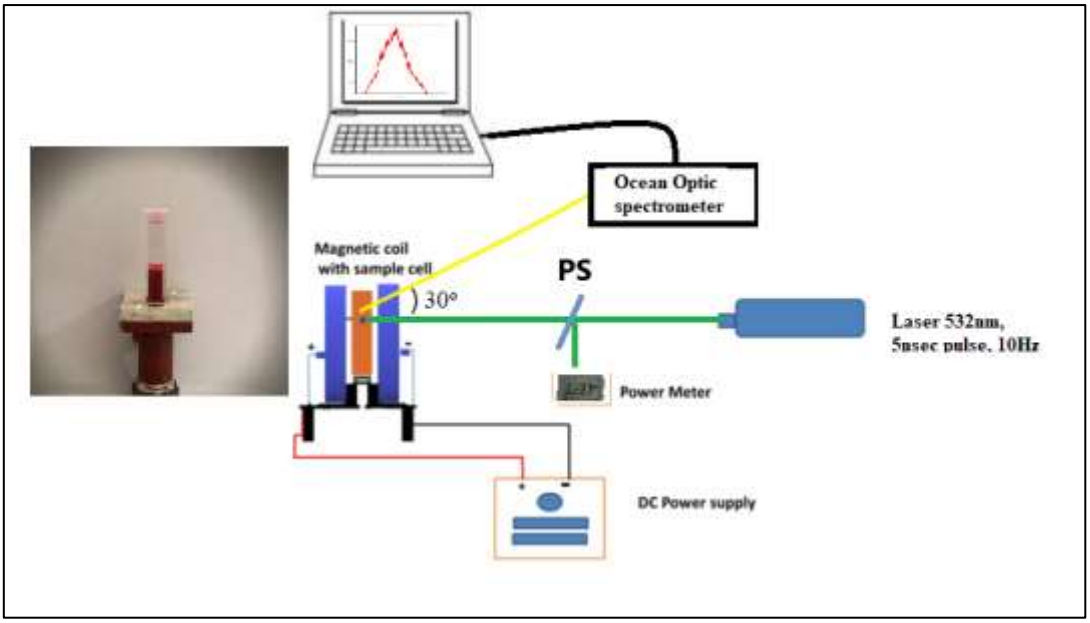

Figure 1. The schematic representation of the optical setup used for controlling the random laser under an external magnetic field in disordered solutions containing dye-doped Fe_3O_4 SNPs.

4. RESULTS AND DISCUSSIONS

4.1. Morphology and Structure of Fe_3O_4 SNPs

Morphological and structural characteristics of the Fe_3O_4 SNPs are shown in **Figure 2**. From the field-emission scanning electron microscopy (FE-SEM) image in **Figure 2(a)**, these SNPs are observed to have spherical-like morphology. According to the inset of **Figure 2(a)**, the size distribution of the SPNs is found to range between 20 and 40 nm. Additionally, the mean size of the Fe_3O_4 SPNs is about 27 nm. The X-ray diffraction (XRD) pattern of the SNPs is depicted in **Figure 2(b)**, indicating the reflections of (220), (311), (400), (422), (511), (440), and (622) planes at 2θ of 30.4, 35.6, 43.5, 53.9, 57.4, 63.0, and 75.0°, respectively (Maarouf *et al.*, 2022). The crystal structure of the SNPs is then confirmed to be from magnetite (Fe_3O_4) without the presence of impurity or secondary peaks. Based on the Scherrer formula (Taylor *et al.*, 1986), the average crystallite size along the main peak (i.e., (311)) is calculated to be about 22 nm, which is following the mean size observed using the FE-SEM analysis.

The Fourier transform infrared (FTIR) spectrum of as-synthesized Fe_3O_4 SNPs is shown in **Figure 2(c)**. The strong absorption band centered at 465 cm^{-1} confirmed that the main phase of the SNPs was magnetite. The peak was attributed to the vibration and torsional modes of Fe-O bonds. It was reported that bulk Fe_3O_4 had the Fe-O absorption band at 570 cm^{-1}. Herein, this band was shifted toward a higher wavenumber since the localized electrons were rearranged on the SNP surface along with an enhanced surface bond force constant (Leong *et al.*, 2016).

The presence of the broad peaks at approximately 1644 and 3446 cm^{-1} was assigned to the bond stretching of O-H and bending vibrations of H_2O molecules, respectively. Due to the formation of Fe_3O_4 SNPs in the aqueous solution, bare and unreacted Fe and O atoms on the SNP surface may bind with OH^- and H^+ respectively, thereby producing a hydroxyl group (-OH). In turn, the resultant hydroxyl group can lead to the surface functionalization of Fe_3O_4 SNPs, arising from its reaction with other positive moieties (Asmara and Kurniawan, 2018).

DOI: https://doi.org/10.17509/ijost.v7i3.51453
p- ISSN 2528-1410 e- ISSN 2527-8045

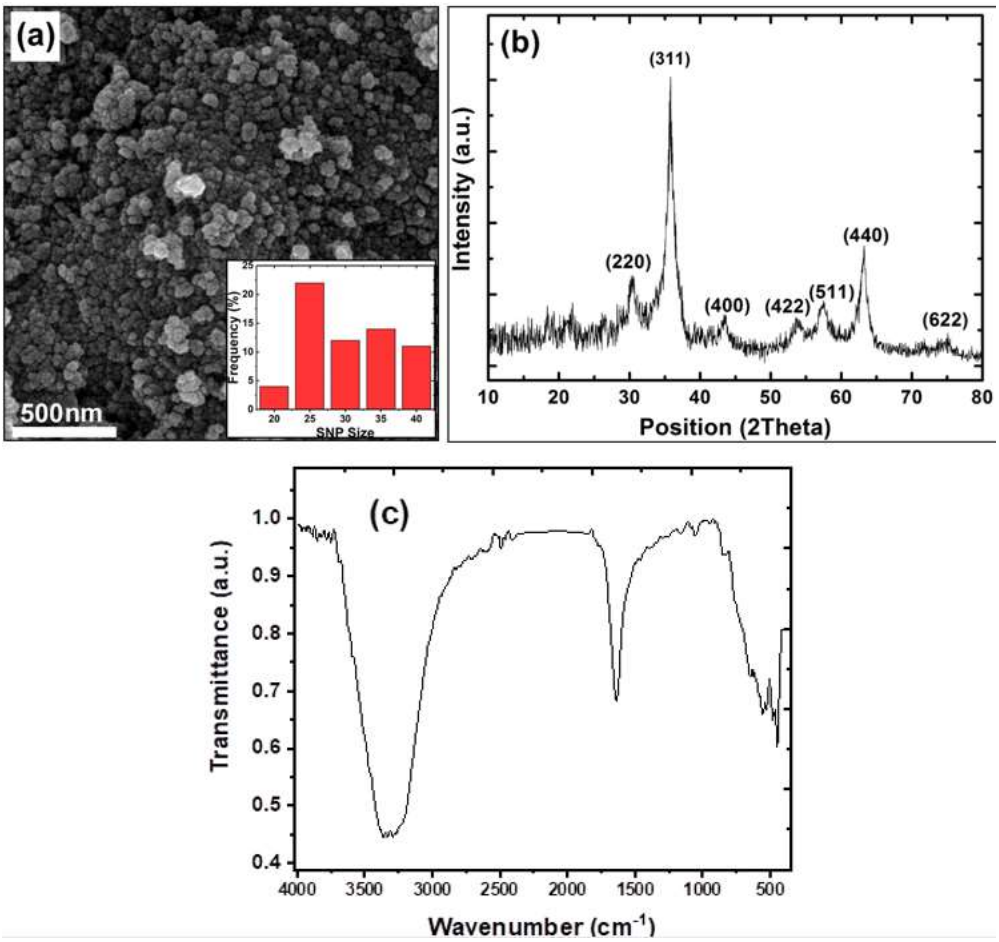

Figure 2. (a) FE-SEM image of Fe_3O_4 SNPs together with the corresponding size histogram as the inset. (b) XRD pattern obtained from Fe_3O_4 SNPs. (c) FTIR spectra of Fe_3O_4 SNPs.

4.2. Absorption and Fluorescence Spectra

The absorption spectra of the samples were measured using a UV-Vis spectrophotometer in the wavelength range of 220–1100 nm. **Figure 3** shows the absorption spectra studied for pure Rh-640 dye with a concentration of 5 mM, pure Fe_3O_4 SNPs with a density of 1.3×10^{17} m^{-3}, and 50% Rh-640:50% Fe_3O_4 mixture. From these results, one can infer that the pure Rh-640 dye possessed a wide absorption spectrum (500–630 nm) with a maximum absorption peak at the wavelength of 540 nm. In the case of the pure Fe_3O_4 SNPs, one can observe that the maximum absorption occurred at the wavelength of 229 nm (Maryanti *et al.,* 2021). Furthermore, the absorption decreased in the wavelength range between 229–800 nm. The spectrum of the dye-Fe_3O_4 SNP mixture was indicative of a reduction and a shift to higher energy (a blue shift), without overlapping with the pump laser wavelength of 532 nm, and the absorption and emission spectra of pure Rh-640 laser and Fe_3O_4 SNPs. In turn, this can lead to the formation of strong scattering centers for the dye-doped SNPs.

Figure 4 shows the comparison between spontaneous emission spectra of pure Rh-640 dye and Rh-640 dye-Fe_3O_4 SNP mixture under pumping energy of 7 mJ recorded using a spectrofluorometer (Shimadzu, RF-5301 PC, Japan). It is observed that the peak of the emission spectrum of pure Rh-640 dye was at the wavelength of 600 nm. The spectrum of the mixture broadened towards a longer wavelength (a red shift) with significant differences in amplitude and bandwidth.

DOI:https://doi.org/10.17509/ijost.v7i3.51453
p- ISSN 2528-1410 e- ISSN 2527-8045

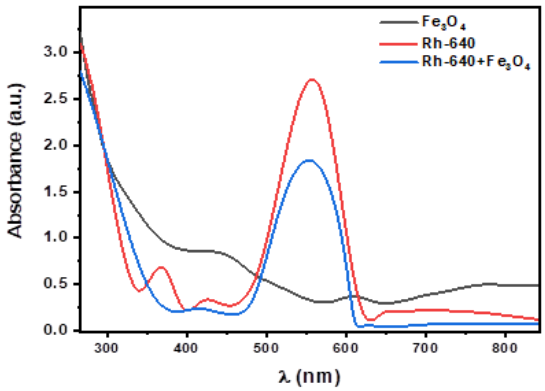

Figure 3. UV-Vi's absorption spectra of pure Rh-640 dye, pure Fe_3O_4, and 50% Rh-640:50% Fe_3O_4 mixture.

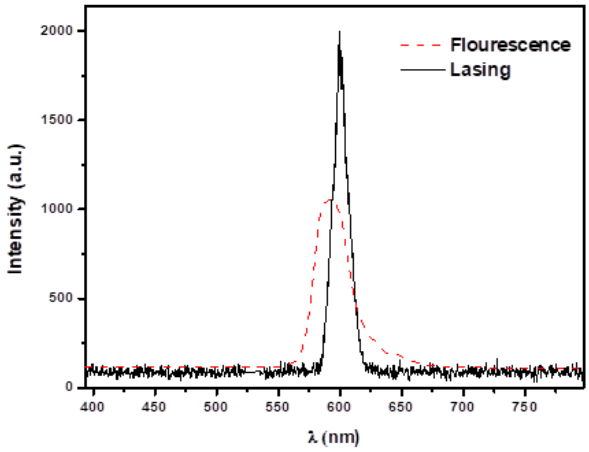

Figure 4. Spontaneous emission spectra of pure Rh-640 dye solution (the dashed red line) and Rh-640: Fe_3O_4 mixture (the solid black line).

4.3. The Effect of Magnetic Field and Concentration

The effect of the magnetic field on laser parameters of Rh-640 dye solution with two different concentrations of Fe_3O_4 SNPs was investigated, and the results obtained are shown in Figures 5 and 6. Figure 5 shows the evolution of emission spectra of sample-1, consisting of 70% Rh-640 (with a concentration 1×10^{-5} M), and 30% Fe_3O_4 SNPs (with a particle density of 2.87×10^{17} cm^{-3}) at different pumping energies (ranging between 1–7 mJ) in the absence and presence of a magnetic field (125 G). Moreover, the peak intensities and full width at half maximum (FWHM) values were extracted as a function of pumping energy.

As inferred from **Figure 5(a)**, no reasonable change in the slope occurred due to the absence of the magnetic field and lower scattering of SNPs. Therefore, a noticeable threshold activity cannot be observed. However, by applying an external magnetic field, a significant change in the threshold energy was seen as it tended to be optimized to surpass the loss and consequently achieve the RL emission (**Figure 5(b)**). Meanwhile, FWHM values changed between 25.2–21.5 nm with increasing the pumping energy from 1 to 7 mJ in the absence of the magnetic field (**Figure 5(c)**). Under the applied magnetic field of 125 G, increasing pumping energy from 1 to 7 mJ decreased the FWHM from 17 to 15 nm (**Figure 5(d)**). Accordingly, the magnetic field and pumping energy influence both FWHM and peak intensities of the emission spectra, and threshold energy.

DOI: https://doi.org/10.17509/ijost.v7i3.51453
p- ISSN 2528-1410 e- ISSN 2527-8045

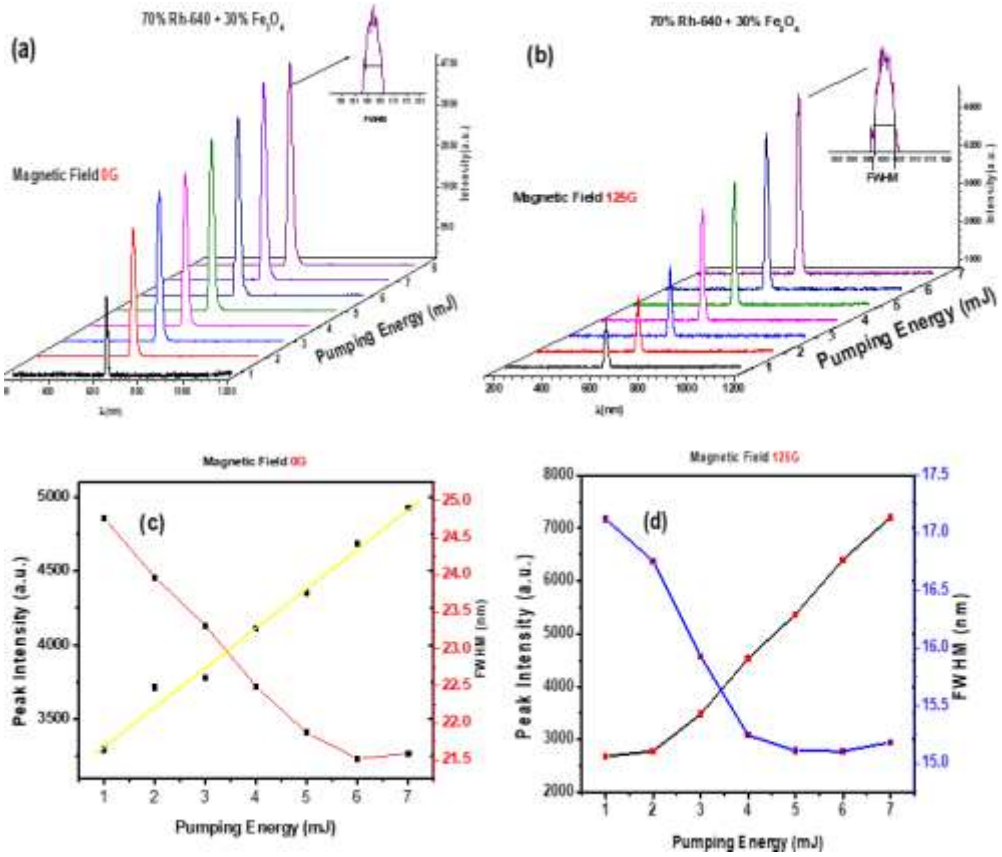

Figure 5. The emission spectra of 70% Rh-640 dye-30% Fe_3O_4 SNP mixture at different pump energies in (a) the absence and (b) the presence of a magnetic field (125 G). The variations of peak intensity and FWHM as a function of pumping energy in (c) the absence and (d) the presence of a magnetic field.

On the other hand, **Figure 6** shows the emission spectra of sample-2, consisting of 50% Rh-640 dye and 50% Fe_3O_4 SNPs at different pump energies (1–7 mJ) in the absence and presence of the magnetic field. Increasing the concentration of scattering centers enhanced the random lasing behavior, followed by the increase in the peak intensity and the narrowing of bandwidth at 0 G and 125 G, respectively (**Figure 6 (a)** and **(b)**). These results indicate that the effects of pumping energy and magnetic field on the random laser parameter (including the emission spectrum intensity and FWHM) for sample-2 (**Figure 6 (c)**) at 0 G were very similar to that explained for sample-1. With the improvement of some parameters, the threshold energy was reduced to 1.89 mJ (**Figure 6 (d)**) whereas it was 2 mJ for the sample at 125 G.

For better clarity, increasing the concentration of scattering centers initiated an improvement in the random lasing behavior, leading to increases in the peak intensity, narrowing of bandwidth, and a decrease in the threshold energy. The higher concentration necessarily leads to a reduction in the scattering mean free path (l_s), which can be calculated using the following relation: $l_s=1/(\rho\sigma)$ (Kamil *et al.,* 2020), where ρ is the particle density and σ is the scattering cross-section. In this way, the l_s of the dye-doped Fe_3O_4 SNPs was calculated to be 14.1 mm for sample-1 and 10.4 mm for sample-2. Essentially, two scattering regimes can exist based on the magnitude of l_s: the weakly scattering regime ($l_s \geq L$) and the diffusive regime ($L > l_s > \lambda$), in which L is the sample size (10 mm) and λ is the emission wavelength (600 nm).

DOI: https://doi.org/10.17509/ijost.v7i3.51453
p- ISSN 2528-1410 e- ISSN 2527-8045

Therefore, l_s values obtained in this study are indicative of dye-doped Fe_3O_4 SNPs with weak scattering behavior. It should be noted that another factor affecting the value of l_s is the magnetic field, according to the literature (Shima *et al.*, 2009). **Tables 1** and **2** show improvements in the value of random laser parameters by changing the magnetic field from 0 to 125 G for the two samples, thereby indicating enhancements in the amplification of the random laser

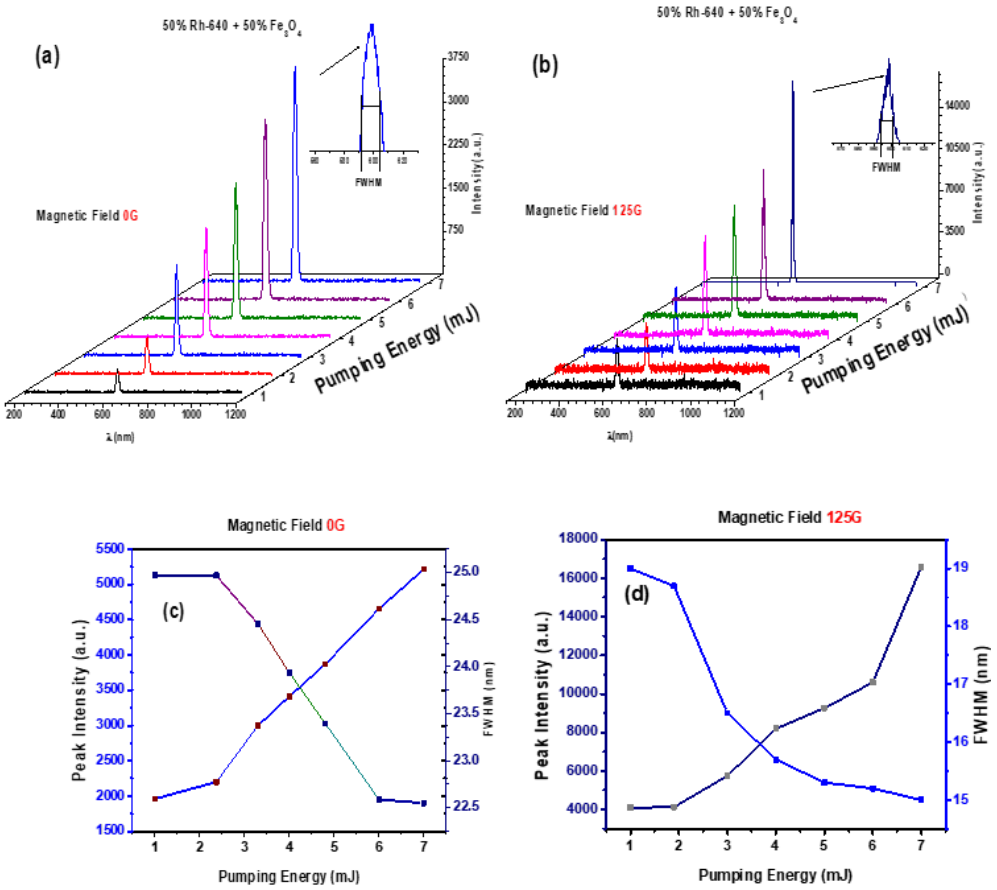

Figure 6. The emission spectra of 50% Rh-640 dye-50% Fe_3O_4 SNP mixture at different pump energies in (a) the absence and (b) the presence of a magnetic field (125 G). The variations of peak intensity and FWHM as a function of pumping energy in (c) the absence and (d) the presence of a magnetic field.

Table 1. Random laser parameters by changing the magnetic field from 0 to 125G (Sample1).

Magnetic field (Gauss)	Threshold pumping energy $_{Pth}$ (mJ)	$FWHM_{below}$ (nm)	$FWHM_{above}$ (nm)
0	3.1	25	21.5
125	2	17.5	15

Table 2. Random laser parameters by changing the magnetic field from 0 to 125G (Sample2).

Magnetic field (Gauss)	Threshold pumping energy $_{Pth}$ (mJ)	$FWHM_{below}$ (nm)	$FWHM_{above}$ (nm)
0	2.8	25	22.5
125	1.89	19.1	15

DOI: https://doi.org/10.17509/ijost.v7i3.51453
p- ISSN 2528-1410 e- ISSN 2527-8045

4.4. The Effect of Response Time on The Emission Wavelength

Generally, the wavelength emission spectra of dye lasers are affected by the concentrations of the scattering centers (NPs), leading to shifts that might be in the direction of red or blue shifts, and a jump from blue to red shifts depending on the NP and dye concentrations (being high, low, or moderate), respectively (Zhang *et al.,* 2017). **Figure 7** shows the investigation of the effect of the response time (0–30 s) on the emission wavelength in the presence of the applied magnetic field (125 G). Red shifts (about 6 nm) took place with increasing the response time from 0 to 25 s. Furthermore, a jump to the blue shift was observed with the increase in the response time from 25 to 30 s. This wavelength shift was supposed to be caused by Fe_3O_4 SNPs that can form chains and change their concentration along the direction of the external magnetic field with increasing response time.

4.5. Transition from Incoherent to Coherent Random Laser

In random laser systems, it is possible to transit from incoherent to coherent modes. This is mainly indicated when spikes appear and their number increases in the corresponding emission spectrum. According to **Figures 5, 6, 7,** and **8(a)**, one can notice the effect of the magnetic field, pumping energy, and the concentration of the dye-doped SNPs on the appearance of the spikes and the increase in their numbers to more than 10 spikes with an FWHM of approximately 1 nm. Alternatively, **Figure 8(b)** shows the following three regions: Region (I), representing the amplified spontaneous emission; and Regions (II) and (III), indicating the change in the intensity of emission spectra and FWHM. The change in Region (II) may represent a transition from the amplified spontaneous emission to the incoherent random laser. Moreover, the occurrence of the super linear change of Region (III) could arise from a transition from incoherent to coherent random laser modes.

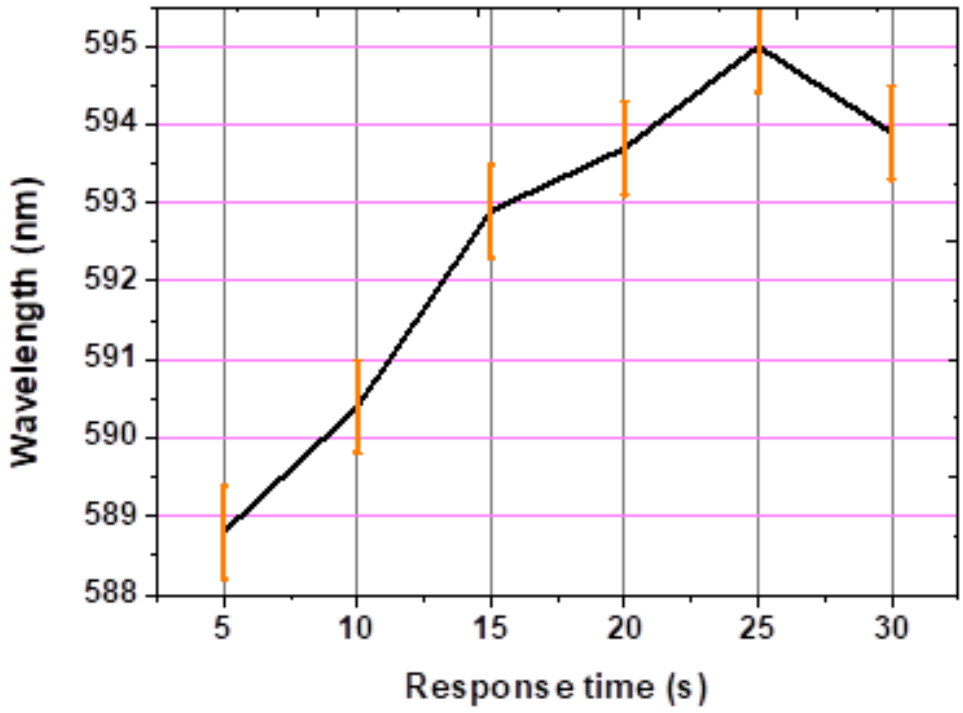

Figure 7. The tuning of wavelength by varying the response time of the magnetic field at constant pumping energy (6mJ/pulse).

DOI: https://doi.org/10.17509/ijost.v7i3.51453
p- ISSN 2528-1410 e- ISSN 2527-8045

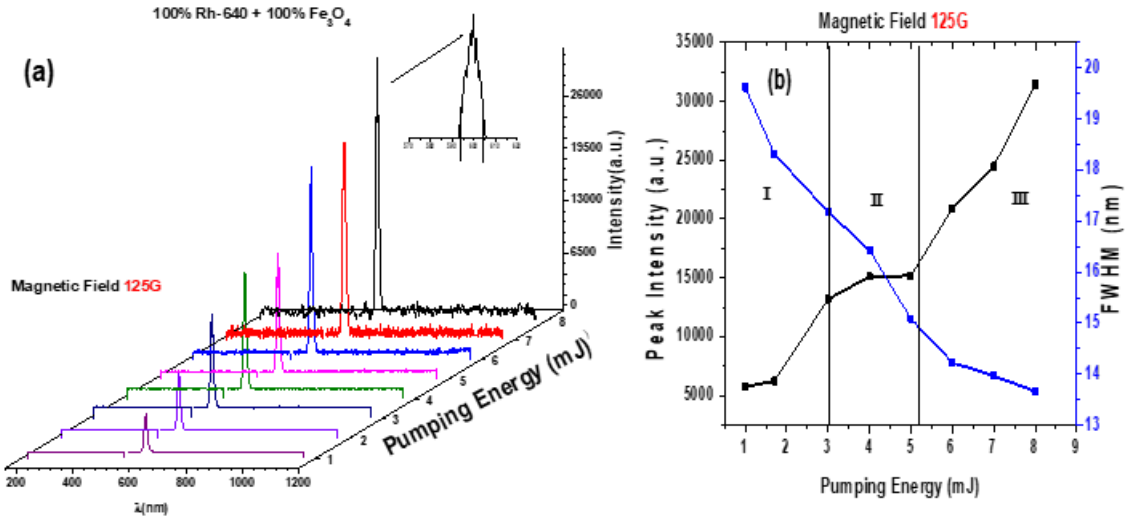

Figure 8. (a) The emission spectra and (b) variations of peak intensity and FWHM as a function of pumping energy in the presence of a constant external magnetic field of 125 G.

5. CONCLUSION

The effect of a relatively weak magnetic field (125 G) on the emission spectra of Rh-640 dye solution containing spherical-like Fe_3O_4 SNPs with an average size of 27 nm was investigated at room temperature. The controllability of the random laser parameters in the presence of the magnetic field was evaluated and confirmed up to acceptable values. Sharp spikes were observed in the emission spectra, resulting from the presence of the applied magnetic field and numerous scattering centers formed by SNPs in the excited region. It was also found that the emission strength increased with increasing the density of the scattering centers. A linear function was established between the spectral shift and the response time (0–30 s) of the magnetic field, allowing for a transition from the amplified spontaneous emission to incoherent random laser as well as from incoherent to coherent random laser modes.

6. ACKNOWLEDGMENT

We thank Prof. S. M. Hamidi from Magneto-plasmonic Lab, Laser and Plasma Research Institute, Tehran, Iran, and Asst. Prof. S. F. Haddaw from the Department of Laser Physics, College of Science for Women, University of Babylon, Hillah, Iraq for helpful advice given in the course of discussion in this work.

7. AUTHORS' NOTE

The author(s) declare(s) that there is no conflict of interest regarding the publication of this article. The authors confirmed that the data and the paper are free of plagiarism.

8. REFERENCES

Asmara, Y. P., and Kurniawan, T. (2018). Corrosion prediction for corrosion rate of carbon steel in oil and gas environment: A review. *Indonesian Journal of Science and Technology*, *3*(1), 64-74.

Bachelard, N., Gigan, S., Noblin, X., and Sebbah, P. (2014). Adaptive pumping for spectral control of random lasers. *Nature Physics*, *10*(6), 426-431.

DOI: https://doi.org/10.17509/ijost.v7i3.51453
p- ISSN 2528-1410 e- ISSN 2527-8045

Bajpai, A. K., and Gupta, R. (2010). Synthesis and characterization of magnetite (Fe3O4)—Polyvinyl alcohol-based nanocomposites and study of superparamagnetism. *Polymer Composites*, *31*(2), 245-255.

Brojabasi, S., Muthukumaran, T., Laskar, J. M., and Philip, J. (2015). The effect of suspended Fe3O4 nanoparticle size on magneto-optical properties of ferrofluids. *Optics Communications*, *336*, 278-285.

Cerdán, L., Costela, A., Durán-Sampedro, G., and García-Moreno, I. (2012). Random lasing from sulforhodamine dye-doped polymer films with high surface roughness. *Applied Physics B*, *108*(4), 839-850.

Chen, S. J., Shi, J. W., Zhai, T. R., Wang, Z. N., Liu, D. H., and Chen, X. (2011). Wavelength variation of a random laser with concentration of a gain material. *Chinese Physics Letters*, *28*(10), 104204.

Chung, M. F., and Fu, C. M. (2011). Optical transmittance and dynamic properties of ferrofluids fe3o4 under dc-biased magnetic fields. *IEEE Transactions on Magnetics*, *47*(10), 3170-3172.

Dai, H. T., Gao, M. N., Xue, Y. X., Xiao, A. X., Ahmad, A., Mohamed, Z., and Feng, S. Z. (2019). Magnetically tunable random lasing from polymer dispersed liquid crystal doped ferromagnetic nanoparticles in capillary. *AIP Advances*, *9*(11), 115015.

Ejbarah, R. A., Jassim, J. M., and Hamidi, S. M. (2020). Random laser action under picosecond laser pumping. *Optical and Quantum Electronics*, *52*(10), 1-8.

Jing, D., Sun, L., Jin, J., Thangamuthu, M., and Tang, J. (2020). Magneto-optical transmission in magnetic nanoparticle suspensions for different optical applications: a review. *Journal of Physics D: Applied Physics*, *54*(1), 013001.

Kedia, S., and Sinha, S. (2017). Random laser emission at dual wavelengths in a donor-acceptor dye mixture solution. *Results in Physics*, *7*, 697-704.

Knitter, S., Kues, M., Haidl, M., and Fallnich, C. (2013). Linearly polarized emission from random lasers with anisotropically amplifying media. *Optics Express*, *21*(25), 31591-31603.

Koo, K. N., Ismail, A. F., Othman, M. H. D., Bidin, N., and Rahman, M. A. (2019). Preparation and characterization of superparamagnetic magnetite (Fe3O4) nanoparticles: A short review. *Malaysian Journal of Fundamental and Applied Sciences*, *15*(1), 23-31.

Kumar, B., Homri, R., Maurya, S. K., Lebental, M., and Sebbah, P. (2021). Localized modes revealed in random lasers. *Optica*, *8*(8), 1033-1039.

Lau, S. P., Yang, H., Yu, S. F., Yuen, C., Leong, E. S., Li, H., and Hng, H. H. (2005). Flexible ultraviolet random lasers based on nanoparticles. *Small*, *1*(10), 956-959.

Leong, Y., Alia, F., and Kurniawan, T. (2016). High temperature oxidation behavior of T91 steel in dry and humid condition. *Indonesian Journal of Science and Technology*, *1*(2), 232-237.

Liao, Y. M., Lai, Y. C., Perumal, P., Liao, W. C., Chang, C. Y., Liao, C. S., and Chen, Y. F. (2016). Highly stretchable label-like random laser on universal substrates. *Advanced Materials Technologies*, *1*(6), 1600068.

DOI: https://doi.org/10.17509/ijost.v7i3.51453
p- ISSN 2528-1410 e- ISSN 2527-8045

Lin, J. H., and Hsiao, Y. L. (2014). Manipulation of the resonance characteristics of random lasers from dye-doped polymer dispersed liquid crystals in capillary tubes. *Optical Materials Express*, *4*(8), 1555-1563.

Maarouf, F. E., Saoiabi, S., Azzaoui, K., Khalil, H., Khalil, M., El Yahyaoui, A., and Sabbahi, R. (2022). Amorphous iron phosphate: Inorganic sol-gel synthesis-sodium and potassium insertion. *Indonesian Journal of Science and Technology*, *7*(2), 187-202.

Maryanti, R., Hufad, A., Nandiyanto, A. B.D., and Tukimin, S. (2021). Teaching the corrosion of iron particles in saline water to students with special needs. *Journal of Engineering Science and Technology*, *16*(1), 601-611.

Meng, X., Fujita, K., Murai, S., and Tanaka, K. (2009). Coherent random lasers in weakly scattering polymer films containing silver nanoparticles. *Physical Review A*, *79*(5), 053817.

Nguyen, M. D., Tran, H. V., Xu, S., and Lee, T. R. (2021). Fe3O4 Nanoparticles: Structures, synthesis, magnetic properties, surface functionalization, and emerging applications. *Applied Sciences*, *11*(23), 11301.

Perumbilavil, S., Piccardi, A., Barboza, R., Buchnev, O., Kauranen, M., Strangi, G., and Assanto, G. (2018). Beaming random lasers with soliton control. *Nature Communications*, *9*(1), 1-7.

Popov, O., Zilbershtein, A., and Davidov, D. (2006). Random lasing from dye-gold nanoparticles in polymer films: Enhanced gain at the surface-plasmon-resonance wavelength. *Applied Physics Letters*, *89*(19), 191116.

Rashidi, M., Li, Z., Jagadish, C., Mokkapati, S., and Tan, H. H. (2021). Controlling the lasing modes in random lasers operating in the Anderson localization regime. *Optics Express*, *29*(21), 33548-33557.

Schönhuber, S., Brandstetter, M., Hisch, T., Deutsch, C., Krall, M., Detz, H., Andrews, A.M., Strasser, G., Rotter, S. and Unterrainer, K. (2016). Random lasers for broadband directional emission. *Optica*, *3*(10), 1035-1038.

Shima, P. D., Philip, J., and Raj, B. (2009). Magnetically controllable nanofluid with tunable thermal conductivity and viscosity. *Applied Physics Letters*, *95*(13), 133112.

Taylor, R. M., Maher, B. A., and Self, P. G. (1986). Magnetite in soils: I. The synthesis of single-domain and superparamagnetic magnetite. *Clay Minerals*, *22*(4), 411-422.

Tommasi, F., Ignesti, E., Lepri, S., and Cavalieri, S. (2016). Robustness of replica symmetry breaking phenomenology in random laser. *Scientific Reports*, *6*(1), 1-8.

Tsai, C. Y., Liao, Y. M., Liao, W. C., Lin, W. J., Perumal, P., Hu, H. H., Lin, S.Y., Chang, C.H., Cai, S.Y., Sun, T.M. and Chen, Y. F. (2017). Magnetically controllable random lasers. *Advanced Materials Technologies*, *2*(12), 1700170.

Turitsyn, S. K., Babin, S. A., Churkin, D. V., Vatnik, I. D., Nikulin, M., and Podivilov, E. V. (2014). Random distributed feedback fibre lasers. *Physics Reports*, *542*(2), 133-193.

Wetter, N., and Jimenez-Villar, E. (2019). Random laser materials: from ultrahigh efficiency to very low threshold (Anderson localization). *Journal of Materials Science: Materials in Electronics*, *30*(18), 16761-16773.

DOI: https://doi.org/10.17509/ijost.v7i3.51453
p- ISSN 2528-1410 e- ISSN 2527-8045

Wiersma, D. S. (2008). The physics and applications of random lasers. *Nature Physics*, *4*(5), 359-367.

Ye, L., Lu, J., Lv, C., Feng, Y., Zhao, C., Wang, Z., and Cui, Y. (2015). Random lasing action in magnetic nanoparticles doped dye solutions. *Optics Communications*, *340*, 151-154.

Ye, L., Zhao, C., Feng, Y., Gu, B., Cui, Y., and Lu, Y. (2017). Study on the polarization of random lasers from dye-doped nematic liquid crystals. *Nanoscale Research Letters*, *12*(1), 1-8.

Yu, S. F. (2015). Electrically pumped random lasers. *Journal of Physics D: Applied Physics*, *48*(48), 483001.

Zhang, H., Feng, G., Zhang, H., Yang, C., Yin, J., and Zhou, S. (2017). Random laser based on Rhodamine 6G (Rh6G) doped poly (methyl methacrylate) (PMMA) films coating on ZnO nanorods synthesized by hydrothermal oxidation. *Results in Physics*, *7*, 2968-2972.

DOI: https://doi.org/10.17509/ijost.v7i3.51453
p- ISSN 2528-1410 e- ISSN 2527-8045